Journal of Applied Polymer Science

Water-Soluble Chitosan Intercalated Montmorillonite Nanocomposites for Removal of Basic Blue 66 and Basic Yellow 1 from Aqueous Solution

Chutima Kaemkit,[1,2] Pathavuth Monvisade,[1,3] Punnama Siriphannon,[1,4] Jiti Nukeaw[1,2]

[1]College of KMITL Nanotechnology, King Mongkut's Institute of Technology Ladkrabang, Ladkrabang, Bangkok 10520, Thailand

[2]Thailand Center of Excellence in Physics, Bangkok 10400, Thailand

[3]Department of Chemistry, Polymer Synthesis and Functional Materials Research Unit, Faculty of Science, King Mongkut's Institute of Technology Ladkrabang, Ladkrabang, Bangkok 10520, Thailand

[4]Department of Chemistry, Faculty of Science, King Mongkut's Institute of Technology Ladkrabang, Ladkrabang, Bangkok 10520, Thailand

Correspondence to: P. Monvisade (E-mail: kmpathav@kmitl.ac.th)

ABSTRACT: Water-soluble chitosan intercalated montmorillonite (wCTS/MMT) nanocomposites were modified and characterized by using Fourier transform infrared, thermogravimetric analysis, and X-ray diffractometer techniques. Two types of wCTS, namely, low molecular-weight chitosan (L-wCTS) and hydroxyethylacryl chitosan (H-wCTS) were synthesized and applied. The batch adsorption experiments on these nanocomposites were conducted by using basic dyes, that is, Basic Blue 66 and Basic Yellow 1 (BY1). The adsorption capacities of sodium montmorillonite (Na-MMT), chitosan, L-wCTS/MMT, and H-wCTS/MMT were measured and compared. The results showed that the adsorption capacities of wCTS/MMT nanocomposites were higher than those values of Na-MMT and chitosan. The adsorption kinetics of wCTS/MMT nanocomposites for BY1 were studied. It was described that the adsorption processes were better fitted by pseudo-second-order equation. The Langmuir and the Freundlich models were used to fit the adsorption isotherm. It was indicated that the adsorption isotherms followed the Langmuir model. The values of the maximum adsorption capacity of L-wCTS/MMT and H-wCTS/MMT adsorbents were at 188.7 and 294.1 mg/g, respectively. © 2012 Wiley Periodicals, Inc. J. Appl. Polym. Sci. 000: 000–000, 2012

KEYWORDS: adsorption, basic dye, langmuir, montmorillonite, water-soluble chitosan

Received 16 March 2012; accepted 24 June 2012; published online

DOI: 10.1002/app.38255

INTRODUCTION

Dye effluents discharged from industries such as paper, textiles, plastic, rubber, leather, cosmetics, and so forth, are the major concerning of aquatic pollution. It regularly persists to degrade with time, sunlight, or biological and chemical treatments. Discharging of dyes into water resources even in a small amount can pose a serious hazard to the aquatic living organisms due to the reduction of light penetration and their toxicity.[1] Several treatment processes for dye removal have been applied extensively such as photocatalytic degradation,[2] sonochemical degradation,[3] cation exchange membranes,[4] electrochemical degradation,[5] chemical–biological degradation,[6] coagulation,[7] and adsorption.[8] Among all those methods, the adsorption of synthetic dyes on efficient solid supports has been considered as a simple and economical method for their removal from wastewater. Various types of adsorbents are effective for removing color from aqueous effluent such as activated carbon,[9,10] zeolite,[9,11] fly ash,[12] chitin and chitosan,[13,14] clay materials,[15–17] and chitosan-modified clay material,[18–20] and so forth.

Chitosan is a natural polysaccharide obtained from the deacetylation of chitin. It is an attractive material and widely used as an adsorbent because of its characteristic advantages such as nontoxicity, hydrophilicity, biocompatibility, biodegradability, antibacterial property, and high sorption capacity.[21] In addition, it has been proved to be used as an effective biosorbent for removing heavy metals[22] and dyes[22,23] from aqueous solutions due to the presence of amino and hydroxyl groups, which can serve as the active sites.[24] Amino groups of chitosan can be cationized, after which they adsorb anionic dyes strongly by electrostatic attraction in the acidic media. Recently, chitosan composites have been developed to adsorb heavy metals and dyes from wastewater because of their remarkably improved

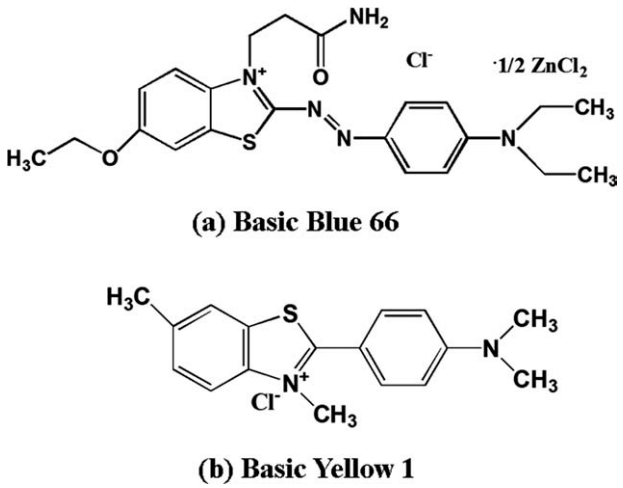

Figure 1. Structure of dyes (a) BB66 (b) BY1.

adsorption capacity. Different kinds of substances have been used to form composites with chitosan such as bentonite,[25] kaolinite,[26,27] and montmorillonite[18,20,27] In our previous study,[20] chitosan/montmorillonite (CTS/MMT) nanocomposite showed good adsorption ability for Basic Blue 9 (BB9), Basic Blue 66 (BB66), and Basic Yellow 1 (BY1). The applications of chitosan are limited because it is insoluble in basic aqueous solutions. Hence, improvement in chitosan solubility can facilitate its applications. However, a literature review showed that the dye removal of water-soluble chitosan (wCTS)/MMT is very scarce through Wang and Wang group,[19] in which they studied the adsorption of Congo Red.

In an attempt to improve the solubility of chitosan in water, many efforts have been made. Hydrogen peroxide can be used to improve the solubility of chitosan by decreasing the molecular weight of chitosan.[28] Furthermore, it is especially interesting in potential due to the presence of amino groups which may be modified by controlling chemical reactions by introducing hydrophilic groups to reactive amino groups.[29–32] In this article, wCTSs were synthesized by two methods, that is, decreasing the molecular weight by using hydrogen peroxide, and the Michael addition reaction of chitosan and hydroxyethylacrylate.[32]

In present study, sodium montmorillonite (Na-MMT) was modified by intercalation with two types of wCTSs to improve the adsorption capability. Adsorption was tested with two basic dyes, that is, BB66 and BY1.

EXPERIMENTAL PROCEDURES

Materials

Chitosan with degree of deacetylation and average molecular weight of about 82.5% and 833 kDa, respectively, was purchased from Eland, Nonthaburi, Thailand. Na-MMT was obtained from Thai Nippon Chemical Industry, Samutsakhon, Thailand, with the cation exchange capacity of 1 mequiv/g. BB66 ($C_{22}H_{28}ClN_5O_2S.0.5ZnCl_2$, dye content ~20 wt %) and BY1 ($C_{17}H_{19}ClN_2S$, dye content ~75 wt %) were purchased from Acros Organics, Morris Plains, New jersey, USA. The chemical structures of those dyestuffs are illustrated in Figure 1. Other reagents were all analytical grade.

Synthesis of Low Molecular-Weight CTS

Low molecular-weight CTS (L-wCTS) was prepared by dissolving 1.0 g of chitosan in 40 mL of 2 wt % acetic acid. Hydrogen peroxide (120 mL of 30% w/v) was then added. The mixture was kept for the hydrolysis reaction at 40°C for 3 h with continuous stirring. After that, 10% NaOH solution was added to adjust pH of the solution to pH 8. The solution was then precipitated by pouring the solution into butanol. The obtained precipitate of L-wCTS was washed several times with methanol and dried in vacuum oven at ambient temperature.

Synthesis of Hydroxyethylacryl Chitosan

Hydroxyethylacryl chitosan (H-wCTS) was prepared by partial referring to the procedure of Ma et al.[32] In details, chitosan (1.0 g) was added into a solution of 1 wt % acetic acid in distilled water (100 mL). Hydroxyethylacrylate (24.0 g) was then added into the solution. The mixture was reacted at 60°C for 48 h with continuous stirring. After cooling down, 10% NaOH was used until pH 8 can be attained. The solution was precipitated by pouring the solution into acetone. The precipitate was washed with plenty of acetone then dried under vacuum at ambient temperature to obtain H-wCTS.

Preparation of Water-Soluble Chitosan Intercalated Montmorillonite

Na-MMT (1.0 g) was dispersed in 40 mL distilled water and then treated in ultrasonic bath (Cole-parmer ultrasonic cleaner, 50/60 Hz and 355/100 W) for 1 h. wCTS (1.0 g) (L-wCTS or H-wCTS) was dissolved in 50 mL of distilled water. The as-prepared wCTS solution was slowly added into the Na-MMT suspension by using peristaltic pump with the rate of about 0.9 mL/min at 60°C with vigorous stirring to obtain L-wCTS/MMT and H-wCTS/MMT nanocomposites. The formed nanocomposites were washed with distilled water until the pH of the supernatant reached 7, then separated by centrifugation at 5000 rpm for 5 min, and dried at 60°C.

Dye Adsorption

Aqueous dye solutions of BY1 and BB66 with an initial concentration of 500 mg/L were prepared. In the adsorption experiment, 1.0 g of absorbents, that is, Na-MMT, chitosan, and wCTS/MMT nanocomposites were added into each 100 mL of the aqueous dye solution, individually. The mixtures were vigorously stirred for 2 h at room temperature and aged overnight.[20] The dye solutions were then separated from the adsorbents by centrifugation at 5000 rpm for 5 min.

The absorbencies of the dye solutions were measured by UV–visible spectrophotometer (PG Instruments, T90 UV/vis spectrometer) at the wavelength of 615 nm for BB66 and 412 nm for BY1. The concentrations of dye solutions were determined by using calibration curve method. The calibration curves of standard solutions of BB66 and BY1 were measured at concentration period of 0.4–90 mg/L in which the absorbance values were in the range of 0.01–0.92. The linear equations were obtained $y = 10.22\ x + 0.0067$, $R^2 = 0.9988$ for BB66 and $y = 30.037\ x + 0.0183$, $R^2 = 0.9999$ for BY1. The amounts of dyes

adsorbed were determined by subtracting the final concentration from the initial concentration of the dye solutions.

The kinetic study experiments for BY1 were performed by batch technique. In each experiment, 100 mL of the 3000 mg/L dye solution was used and 1.0 g of wCTS/MMT was added as an adsorbent. The contact times were applied from 5 to 1440 min, during those times, the adsorption equilibrium was reached and the maximum of dye removal was attained. The concentration of dye left in each solution was measured by UV–visible spectrophotometer.

The experimental data were fitted with two simplified kinetic models including pseudo-first-order and pseudo-second-order equations. These two equations were analyzed to describe the adsorption processes of BY1. The pseudo-first-order equation[33] can be expressed as

$$\log(q_e - q_t) = \log q_e - \frac{k_1 t}{2.303} \quad (1)$$

Where k_1 is the pseudo-first-order rate constant (min^{-1}), q_e and q_t are the amounts of dyes adsorbed (mg/g) at equilibrium and at time t (min). The plot of $\log(q_e - q_t)$ versus t gives a straight line for the pseudo-first-order adsorption kinetics. The values of the pseudo-first-order rate, k_1 were obtained from the slopes of the straight lines. The pseudo-second-order equation[34] is expressed as

$$\frac{t}{q_t} = \frac{1}{k_2 q_e^2} + \frac{t}{q_e} \quad (2)$$

Where k_2 (g mg^{-1} min^{-1}) is the rate constant of pseudo-second-order adsorption. The plot of t/q_t versus t gives a linear relationship, which allows the values of q_e and k_2 obtained from the slope and intercept of the straight lines, respectively.[35,36]

Isotherm experiments for BY 1 were undertaken in a batch equilibrium technique. A sample wCTS/MMT (1.0 g) was used with a 100-mL aqueous dye solution by using the concentrations of the aqueous dye solution 500–7000 mg/L and adsorption time of 1440 min. The concentration of dye left in each solution was measured by UV–visible spectrophotometer.

The adsorption isotherm data were analyzed by fitting them to both of the Langmuir[37] and the Freundlich[38] isotherm models to find the suitable model. The Langmuir and the Freundlich adsorption parameters were determined using eqs. (3) and (5), respectively. The Langmuir equation is expressed as

$$\frac{C_e}{q_e} = \frac{1}{K_L q_m} + \frac{C_e}{q_m} \quad (3)$$

where C_e (mg/L) is the equilibrium concentration of the dye, q_e (mg/g) is the equilibrium amount of the dye adsorbed per unit weight of adsorbent, q_m (mg/g) is the maximum amount of dye adsorbed per unit weight of adsorbent to form a complete monolayer coverage, and K_L (L/mg) is the Langmuir adsorption constant. The constants can be evaluated from the intercepts and the slopes of the linear plots of C_e/q_e versus C_e.

The Freundlich equation is expressed as

$$q_e = K_f C_e^{1/n} \quad (4)$$

$$\log q_e = \log K_F + \frac{1}{n} \log C_e \quad (5)$$

where capacity constant, K_f and n are the Freundlich constants related to adsorption capacity and adsorption intensity, respectively. In case of $n = 1$ indicates linear adsorption and equal adsorption energies for all sites. Values of n between 2 and 10 indicate good adsorption. However, $n < 1$ shows that the marginal adsorption energy decreased with increasing surface concentration.[35,36]

Characterization

Fourier transform infrared (FTIR) spectra of L-wCTS, H-wCTS, Na-MMT, and wCTS/MMT nanocomposites were characterized using a FTIR spectrophotometer (FTIR, Perkin Elmer FTIR Spectrum GXA) in potassium bromide (KBr) pellet method. FTIR spectra were collected over a range of 400–4000 cm^{-1}. The interlayer space between platelets of the Na-MMT and wCTS/MMTs were studied at room temperature using X-ray diffractometer (XRD, D8 ADVANCE X-ray diffractometer), starting from 2θ of 1–25°. Samples of L-wCTS, H-wCTS, Na-MMT, and wCTS/MMTs were characterized using thermogravimetric analysis (TGA, TGA 2950 thermobalance, TA Instruments). The samples were heated from 50–900°C with a heating rate of 20°C/min under air condition. Average molecular weight of chitosan and L-wCTS were determined by gel permeation chromatography (GPC, Waters 600E). Pullulans standard was first injected into the ultrahydrogel linear column of GPC equipped with refractive index detector. The solution of samples in buffer of 0.5*M* CH_3COOH/0.5*M* CH_3COONa were eluted through column with 20-μL injection volume at a flow rate of 0.6 mL/min using the same buffer as eluent. The column and detector were both set at the temperature of 30°C.[39]

RESULTS AND DISCUSSION

Characterization of L-wCTS and H-wCTS

The weight average molecular weight of L-wCTS was reduced from 833 kDa of chitosan to 6.5 kDa. This can be confirmed that the chain of the chitosan was hydrolyzed by hydrogen peroxide. The solubility of L-wCTS and H-wCTS in distilled water comparing with chitosan was evaluated at a concentration of 20 mg/mL at various temperatures from room temperature to 100°C. The results showed that L-wCTS could completely dissolve in distilled water at 100°C, whereas H-wCTS could dissolve in distilled water at 70°C, in which the chitosan cannot dissolve in distilled water at all range of temperature.

FTIR spectra of chitosan, L-wCTS, and H-wCTS are shown in Figure 2. The chitosan and L-wCTS have the same signals at about 3430 cm^{-1} for O—H stretching and N—H stretching region, peak at about 2920 cm^{-1} is attributed to C—H stretching, and 1650 and 1590 cm^{-1} regions for N—H bending vibration, 1420 and 1370 cm^{-1} for C—H bending, and 1150 and 1080 cm^{-1} for C—O stretching.[20] However, hydrogen peroxide was proved to be an efficient tool for chitosan degradation in this work. The mechanism was suggest from the literature[40] that H-abstraction from C-1, C-2, C3, C-4, or C-5 of a glucosamine unit leads to scission of the glycosidic bond which could be

Applied Polymer SCIENCE

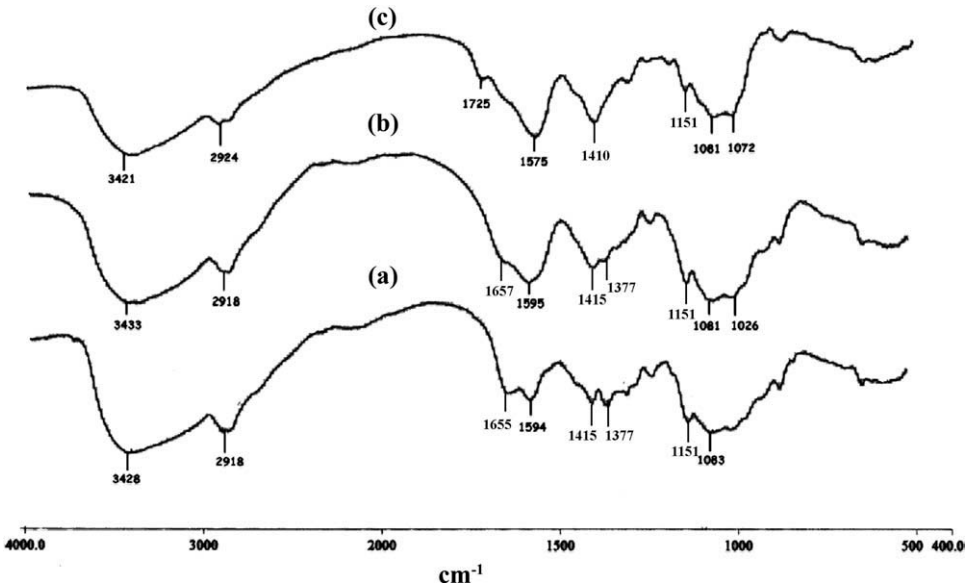

Figure 2. FT-IR spectra of (a) Chitosan, (b) L-wCTS, and (c) H-wCTS.

further oxidized to produce carboxylic acid. In addition, the spectral profiles and relative intensities of the bonds exhibited correlation with mechanism of H-abstraction from C-1, C-2, C3, C-4, or C-5 of a glucosamine unit. H-abstraction formed at C-2 resulting in the cleavage of the glycosidic bond is also proposed. H-abstraction from C-1 to C-3 and possibly the amino group leads to the deamination of 2-amino-2-deoxy-D-glucose. The increase of carboxyl group content in degraded chitosan was in close relation to the deamination, suggesting that the scission of glycosidic bond was predominantly from H-abstraction at C-1 and C-2 that both led to the deamination. Some splitting of C—C bonds within sugar residues also occurred, which led to ring-opening oxidation and formation of carboxyl groups. However, the change was difficult to see clearly by FTIR as reported by Qin et al.[40]

The FTIR spectra of H-wCTS are also showed all peaks appeared in the FTIR spectra, excluding the chitosan and L-wCTS at the peak of 1725 cm^{-1} which indicated C=O stretching of part of hydroxyethylacrylate group. At this point, it confirmed that the H-wCTS was modified by introducing hydrophilic groups to reactive amino groups.

Characterization of wCTS/MMT Nanocomposites

The d_{001}-spacing of Na-MMT and wCTS/MMTs was determined by XRD. The XRD patterns of Na-MMT and wCTS/MMTs are shown in Figure 3. The crystalline peak corresponded to 001 plane of the Na-MMT was at $2\theta = 7.12°$, $d_{001} = 1.24$ nm.[20,41–43] The XRD pattern of the initial chitosan exhibited its characteristic peak at $2\theta = 10.3°$, indicating the crystallinity of chitosan, which reported previously.[32] After modification of Na-MMT with wCTS, the d_{001} peak shifted to the lower angles for both modified with L-wCTS and H-wCTS which were at 2θ around $3.88°$ (d_{001} ~2.26 nm) and $5.96°$ (d_{001} ~1.48 nm), and 2θ around $6.72°$ ($d_{001} = 1.32$ nm) and $3.32°$ ($d_{001} = 2.66$ nm), respectively. Those broad reflections around 2θ ~$5.96°$ (d_{001} ~1.48 nm) and $6.72°$ ($d_{001} = 1.32$ nm) were assumed to be monolayer of intercalated wCTS in MMT [Figure 4(a)], whereas 2θ around $3.88°$ (d_{001} ~2.26 nm) and $3.32°$ ($d_{001} = 2.66$ nm) were related to the bilayer intercalation of wCTS in MMT [Figure 4(b)].[20] These shifting indicated the intercalation of L-wCTS or H-wCTS into the interlayers of the Na-MMT,

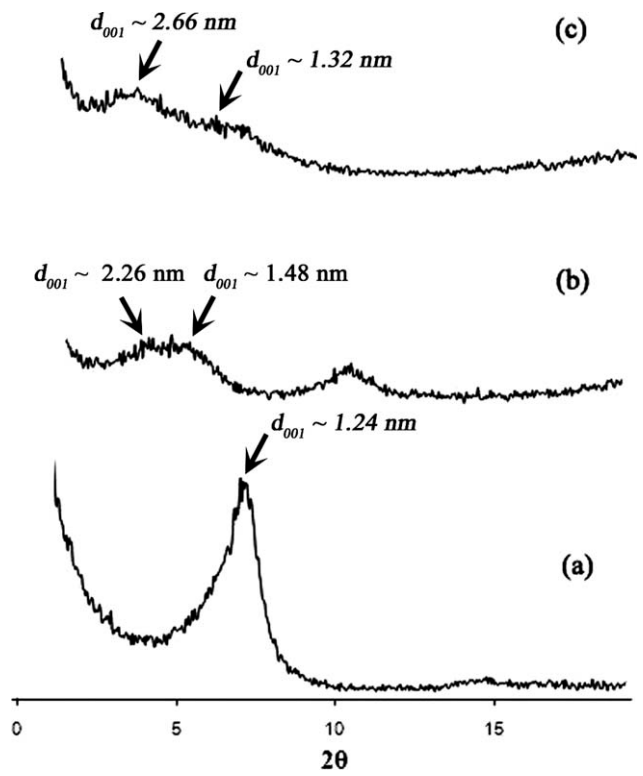

Figure 3. XRD patterns of (a) Na-MMT, (b) L-wCTS/MMT, and (c) H-wCTS/MMT.

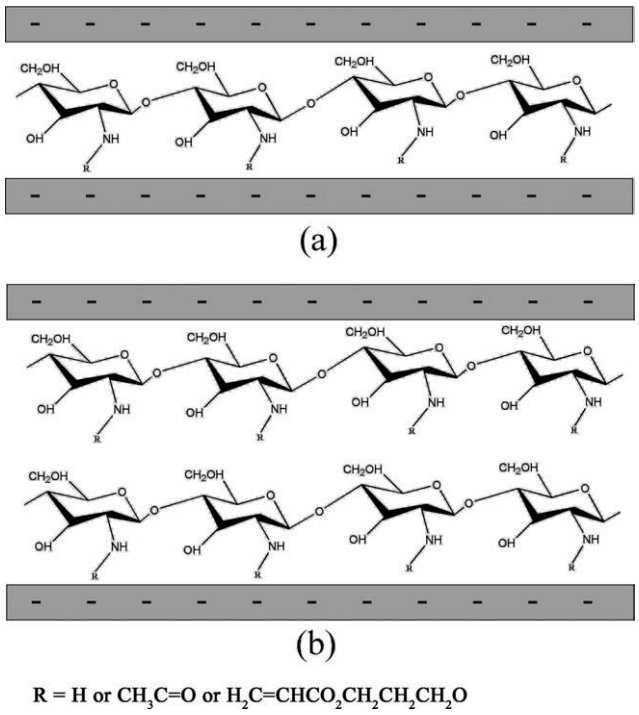

Figure 4. Intercalation of wCTS into Na-MMT (a) monolayer and (b) bilayer structures.

bringing about the expansion of the basal spacing of the MMT layers. However, the XRD pattern of L-wCTS/MMT showed characteristic peak at $2\theta = 10.3°$. Thus, L-wCTS was assumed that crystal form. Whereas, the peak at $2\theta = 10.3°$ of H-wCTS/MMT disappeared. Hence, H-wCTS could be amorphous. The lower crystallinity of H-wCTS ascribed to the presence of hydroxyethylacryl moiety which might hindered the formation of inter-and extramolecular hydrogen bonds after chemical modification.[32]

The FTIR spectra of Na-MMT [Figure 5(a)] show the vibration bands at about 3620 cm^{-1} for O—H stretching, 3440 cm^{-1}due to interlayer and intralayer H-bonded O—H stretching, at 1640 cm^{-1} vibration indicated harmonic band of O—H from adsorbed water, at 1090–1040 cm^{-1} for Si—O stretching, 916 and 620 cm^{-1} Al—OH, 843 and 795 cm^{-1} due to (Al, Mg)—OH vibration and 520 and 470 cm^{-1} for Si—O—Si bending.[20] While the spectra of wCTS/MMT nanocomposites [Figure 5(b, c)] showed the correlation peaks of Na-MMT [Figure 5(a)] and wCTS [Figure 2(b, c)]. The identified peaks of wCTS show at about 3420 cm^{-1} for O—H stretching and N—H stretching region, 2910 and 1590 cm^{-1} regions representing to C—H stretching and the overlapping between C—H bending and N—H bending vibration, respectively. Another peak appears only in the spectrum of H-wCTS/MMT at 1725 cm^{-1} attributed to C=O stretching belonging to H-wCTS. These spectra of the L-wCTS/MMT and H-wCTS/MMT indicate the combination of characteristic absorptions due to the wCTS and Na-MMT.

The moisture, organic, and ash content was determined by TGA. The first range (50–200°C) was associated with the loss of water, whereas the second range (200–450°C) corresponded to organic content. There was another step (450–900°C), which may be assigned to the oxidative degradation of carbonaceous residue and inorganic content (ash content) as the values are shown in Table I. It could be noted that the organic and ash

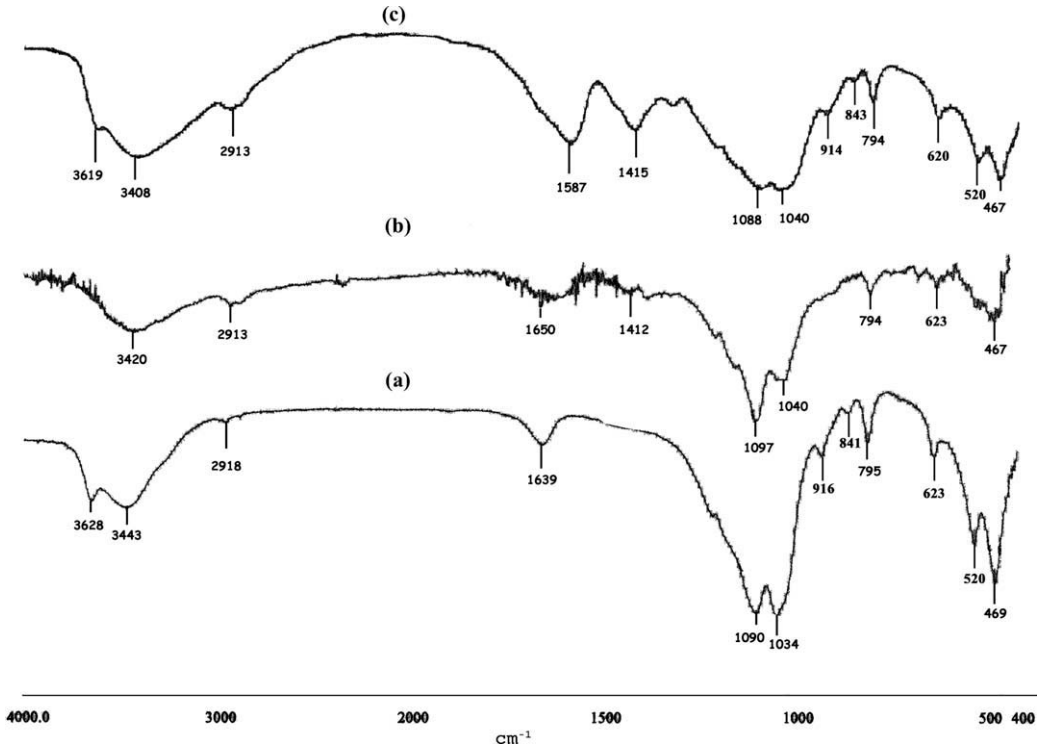

Figure 5. FT-IR spectra of (a) Na-MMT, (b) L-wCTS/MMT, and (c) H-wCTS/MMT.

Table I. Percentage of Composition, Percentage of dye Removal, and Adsorption Capacity of Na-MMT, L-wCTS, H-wCTS, and L-wCTS/MMT and H-wCTS/MMT Nanocomposites

	% Weight from TGA			Dyes			
				Basic Blue 66		Basic Yellow 1	
Adsorbent	Moisture content	Organic content	Ash content	% Removal	Adsorption capacity (mg/g)	% Removal	Adsorption capacity (mg/g)
MMT	8	6	86	87.0	43.5	74.6	37.3
Chitosan	11	85	4	60.0	30.0	22.8	11.4
L-wCTS	10	81	9	N/A[a]	N/A	N/A	N/A
H-wCTS	25	58	17	47.0	23.5	52.0	26.0
L-wCTS/MMT	5	53	42	99.6	49.8	99.6	49.8
H-wCTS/MMT	12	38	50	96.0	48.0	96.8	48.4

[a]Not applicable.

contents in the wCTS/MMT nanocomposites related to the contents of wCTS and MMT, respectively, in the nanocomposites. As seen in Table I, the organic contents of L-wCTS/MMT and H-wCTS/MMT were 53 and 38 wt %, respectively, suggesting the higher content of L-wCTS than the content of H-wCTS in the nanocomposites.

Effect of Different Types of wCTS/MMT on Dye Adsorption

The dye adsorption ability of Na-MMT, Chitosan, L-wCTS/MMT, and H-wCTS/MMT nanocomposites at 500 mg/L of initial dye solution concentration of BB66 and BY1 is shown in Table I. The experimental data show the excellent adsorption ability of L-wCTS/MMT and H-wCTS/MMT nanocomposites over those of Na-MMT and H-wCTS powder. From Table I, it was seen that Na-MMT, chitosan, and H-wCTS powder can adsorb BB66 at 87.0, 60.0, and 47.0% leading to the adsorption capacities of 43.5, 30.0, and 23.5 mg/g, respectively. For BY1, it was adsorbed by Na-MMT, chitosan, and H-wCTS powder at 74.6, 22.8, and 52.0%, referring to the adsorption capacities of 37.3, 11.4, and 26.0 mg/g, respectively. However, the adsorption ability of L-wCTS for these dye solutions cannot be evaluated because some part of L-wCTS dissolved in the dye solutions bringing about the shifting in λ_{max} of UV absorbance of dye solutions. After modification, L-wCTS/MMT and H-wCTS/MMT nanocomposites show the improvement of the dye adsorption up to 99.6% for both BB66 and BY1, corresponding to the adsorption capacities up to 49.8 mg/g. It is suggested that the intercalation of L-wCTS or H-wCTS, as appropriate, into the interlayer spaces of Na-MMT, as supported by XRD analysis, could enlarge the d_{001}-spacing of Na-MMT, facilitating the penetration of the basic dyes.

Adsorption Kinetics

Effect of the contact times on the adsorption capacities of BY1 by L-wCTS/MMT and H-wCTS/MMT nanocomposites was investigated and the results are shown in Figure 6(a). It can be seen that adsorption capacity of H-wCTS/MMT increased rapidly within 10 min, then, reached equilibrium. While the adsorption capacity of L-wCTS/MMT sharply increased with relatively longer time within 120 min and then gradually increased with prolonging the contact time until reached equilibrium. It was due to the wider expansion of the MMT interlayer spacing of H-wCTS/MMT (d_{001} = 2.66 nm) than that of L-wCTS/MMT (d_{001} = 2.26 nm), as stated in the XRD analysis. This larger expansion brought about the larger pore size of H-wCTS/MMT,

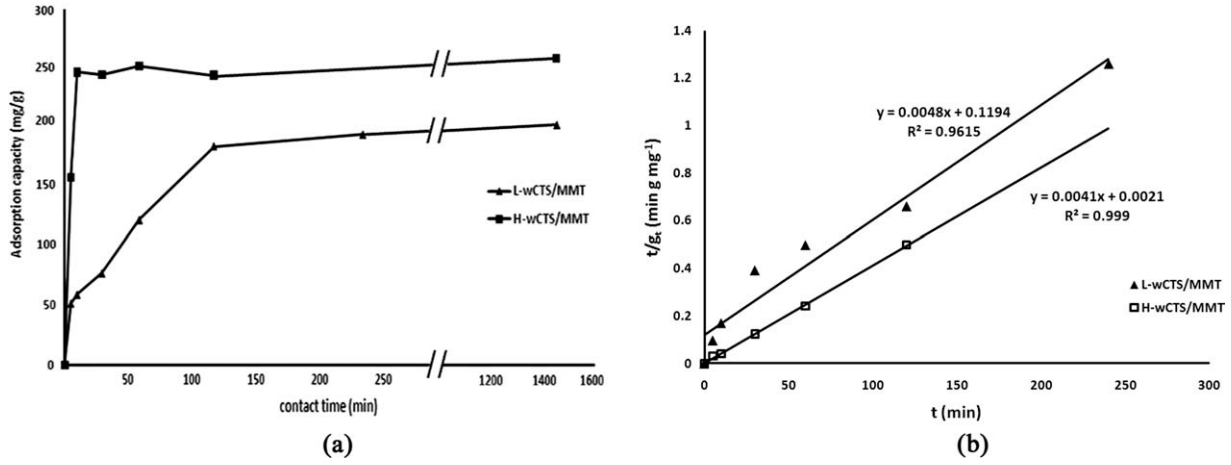

Figure 6. (a) Effect of the contact time on adsorption capacity of L-wCTS/MMT and H-wCTS/MMT nanocomposites for BY1 and b) pseudo-second-order models for the adsorption of BY1 by L-wCTS/MMT and H-wCTS/MMT nanocomposites.

Table II. Pseudo-Second Order Kinetic Parameter and Langmuir Isotherm Constants for the Adsorption Basic Yellow 1 onto wCTS/MMT Nanocomposites

	Pseudo-second order			Langmuir isotherm constants		
Adsorbent	k_2	q_e, calculated (mg/g)	R^2	q_m (mg/g)	K_L	R^2
L-wCTS/MMT	0.0048	0.1194	0.9615	188.67	0.1360	0.9969
H-wCTS/MMT	0.0041	0.0021	0.9999	294.11	0.2178	0.9949

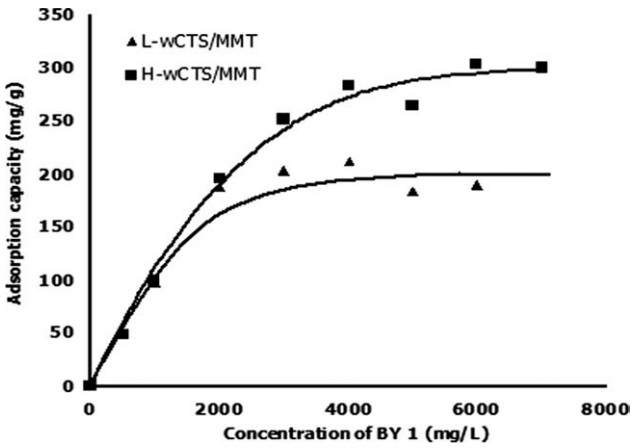

Figure 7. Effect of the dye concentration on adsorption capacity of L-wCTS/MMT and H-wCTS/MMT nanocomposites for BY1.

facilitating the easier penetration of BY1 (molecular diameter ~3.5 ± 0.5 nm)[44] into the interlayer space of the nanocomposites, as such, rapidly reached the adsorption equilibrium of H-wCTS/MMT.

The experimental data were fitted with two simplified kinetic models including pseudo-first-order and pseudo-second-order equations. These equations were analyzed to describe the adsorption processes of BY1. The plot of $\log(q_e - q_t)$ versus t gives a straight line for the pseudo-first-order adsorption kinetics. The values of pseudo-first-order rate, k_1, obtained from the slopes of the straight line. The plot of t/qt versus t give a linear relationship for pseudo-second-order adsorption kinetics, which allows the values of q_e and k_2 can be obtained from the slope and intercept of the straight lines, respectively. The results of regression analysis were fitted well with the pseudo-second-order adsorption equation as shown in Figure 6(b), which showed high correlation coefficients (R^2) at 0.9615 and 0.9990 for L-wCTS/MMT and H-wCTS/MMT, respectively. The kinetic parameters for all experimental data were given in Table II. These results indicated that the adsorption rate of BY1 depended on both of the concentration of dye at the adsorbent surface and the adsorbance of these adsorbed at equilibrium.

Adsorption Isotherms

Figure 7 typically shows the influence of initial dye concentration on adsorption capacity of L-wCTS/MMT and H-wCTS/MMT nanocomposites. For L-wCTS/MMT, the adsorption capacity of the nanocomposites sharply increased from 49.7 to 188.0 mg/g, as the initial dye concentration increased from 500 to 2000 mg/L, and slightly increased beyond those concentrations. Similarly, the adsorption capacity of H-wCTS/MMT sharply increased from 48.4 to 282.8 mg/g, which the initial dye concentration increased from 500 to 4000 mg/L, and slightly increase later up to 302.8 mg/g.

The adsorption isotherms of BY1 by using L-wCTS/MMT and H-wCTS/MMT nanocomposites were determined. The adsorption isotherm data were analyzed by fitting to both of the Langmuir[37] and the Freundlich[38] isotherm models to find the suitable model. The parameters belonging to the adsorption isotherm models were given in Table II.

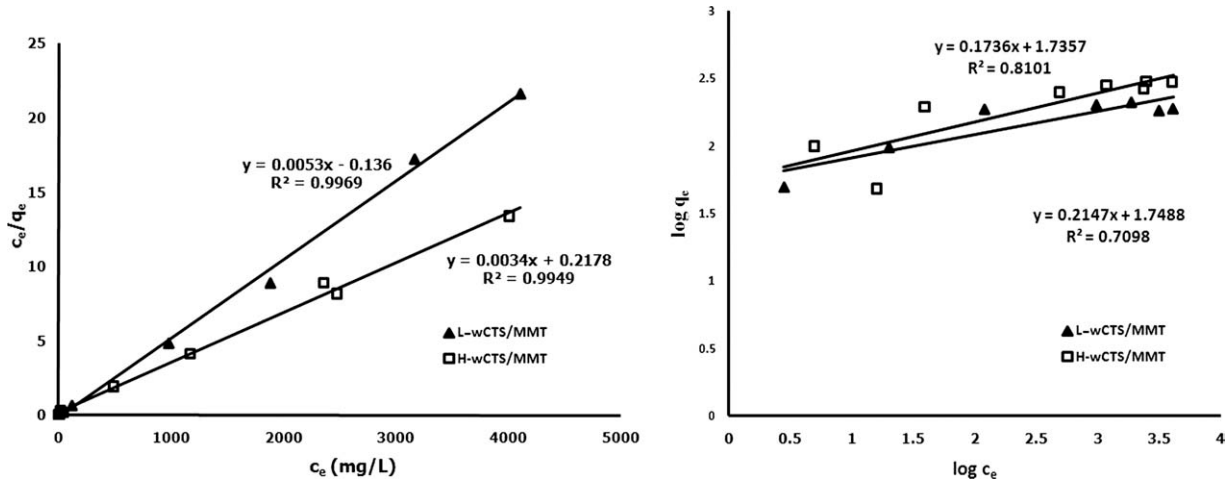

Figure 8. The adsorption isotherms of L-wCTS/MMT and H-wCTS/MMT nanocomposites for BY1 a) Langmuir isotherms and b) Freundlich isotherms.

The Langmuir adsorption isotherms for the adsorption of BY1 on L-wCTS/MMT and H-wCTS/MMT nanocomposites are shown in Figure 8(a). The values of the correlation coefficient (R^2) at 0.9969 and R^2 at 0.9949 clear that the adsorption curve are linear with the linearization of the equations of $y = 0.0053x + 0.136$ for L-wCTS/MMT and $y = 0.0034x + 0.2178$ for H-wCTS/MMT, respectively. The fact that the Langmuir isotherm fits the experimental data suggested the monolayer coverage of the dye on the surface of the nanocomposites. Moreover, from the Langmuir isotherm, the maximum adsorption capacity, q_m, (mg of dye per g of adsorbent) of H-wCTS/MMT adsorbent was 294.1 mg/g, which was higher than that of L-wCTS/MMT adsorbent (188.7 mg/g). This was due to the larger expansion of the basal spacing of H-wCTS/MMT than that of L-wCTS/MMT, as confirmed by the shifting of their characteristic peak positions in the XRD analysis. This intercalation brought about the larger pore size of H-wCTS/MMT, facilitating the more penetration of BY1 into the interlayer space of the nanocomposites. Thus, the higher q_m could be obtained for H-wCTS/MMT.

In case of Freundlich model, the values of R^2 for L-wCTS/MMT and H-wCTS/MMT nanocomposites are at 0.7098 and 0.8101, respectively [Figure 8(b)]. Therefore, the adsorption of BY1 on these nanocomposites does not obey the Freundlich isotherm.

CONCLUSION

Two types of wCTS/MMT nanocomposites, that is, L-wCTS/MMT and H-wCTS/MMT were prepared by intercalation of appropriate wCTS into Na-MMT. The adsorptions of basic dyes, that is, BB66 and BY1 by wCTS/MMT nanocomposites were carried out and the results showed that the nanocomposites exhibited the higher adsorption capacity than the Na-MMT and chitosan. The kinetic mechanism and isotherm studies of BY1 on wCTS/MMT nanocomposites followed the pseudo-second-order model and the Langmuir model, respectively. The maximum adsorption capacities of L-wCTS/MMT and H-wCTS/MMT nanocomposites for BY1 were at 188.7 and 294.1 mg/g, respectively. Consequently, H-wCTS/MMT shows the higher adsorption performance than L-wCTS/MMT as it can rapidly reach adsorption equilibrium by 10 min with high maximum adsorption capacity.

ACKNOWLEDGMENTS

This work has partially been supported by the National Nanotechnology Center (NANOTEC), NSTDA, Ministry of Science and Technology, Thailand, through its program of Center of Excellence Network. The authors would like to thank the Scientific Instruments Service Center, Faculty of Science, King Mongkut's Institute of Technology Ladkrabang, Thailand, for XRD, XRF, and TGA analyses. Thanks also to the National Metal and Materials Technology Center, National Science and Technology Development Agency for GPC analysis.

REFERENCES

1. Ramakrishna, K. R.; Viraraghavan, T. *Water. Sci. Technol.* **1997,** *36*, 189.
2. Sohrabi, M. R.; Ghavami, M. *J. Hazard. Mater.* **2008,** *153*, 1235.
3. Abbasi, M.; Asl, N. R. *J. Hazard. Mater.* **2008,** *153*, 942.
4. Wu, J. S.; Liu, C. H.; Chu, K. H.; Suen, S. Y. *J. Membr. Sci.* **2008,** *309*, 239.
5. Fan, L.; Zhou, Y.; Yang, W.; Chen, G.; Yang, F. *Dyes Pigm.* **2008;***76*:440.
6. Sudarjanto, G.; Keller-Lehmann, B.; Keller, J. *J. Hazard. Mater.* **2006,** *138*, 160.
7. Verma, A. K.; Dash, R. R.; Bhunia, P. *J. Environ. Manage.* **2012,** *93*, 154.
8. Rafatullah, M.; Sulaiman, O.; Hashim, R.; Ahmad, A. *J. Hazard. Mater.* **2010,** *177*, 70.
9. Meshko, V.; Markovska, L.; Mincheva, M.; Rodrigues, A. E. *Water Res.* **2001,** *35*, 3357.
10. Rozada, F.; Calvo, L. F.; Garcia, A. I.; Martin-Villacorta, J.; Otero, M. *Bioresour. Technol.* **2003,** *87*, 221.
11. Wang, S.; Li, H.; Xu, L. *J. Colloid Interface Sci.* **2006,** *295*, 71.
12. Janos, P.; Buchtova, H.; Ryznarova, M. *Water Res.* **2003,** *37*, 4938.
13. Ravi Kumar, M. N.V. *React. Funct. Polym.* **2000,** *46*, 1.
14. Chiou, M. S.; Ho, P. Y.; Li, H. Y. *Dyes Pigm.* **2004,** *60*, 69.
15. Gemeay, A. H.; Sherbiny, E. I.; Zaki, A. B. *J. Colloids Interface Sci.* **2002,** *245*, 116.
16. Gemeay, A. H. *J. Colloids Interface Sci.* **2002,** *251*, 235.
17. Wang, C. C.; Juang, L. C.; Hsu, T. C.; Lee, C. K.; Lee, J. F.; Huang, F. C. *J. Colloids Interface Sci.* **2004,** *273*, 80.
18. Wang, L.; Wang, A. *J. Hazard. Mater.* **2007,** *147*, 979.
19. Wang, L.; Wang, A. *Chem. Eng. J.* **2008,** *143*, 43.
20. Monvisade, P.; Siriphannon, P. *Appl. Clay Sci.* **2009,** *42*, 427.
21. Rinaudo, M. *Prog. Polym. Sci.* **2006,** *31*, 603.
22. WanNgah, W. S.; Teong, L. C.; Hanafiah, M. A. K. M. *Carbohydr. Polym.* **2011,** *83*, 1446.
23. Mahmoodi, N. M.; Salehi, R.; Arami, M.; Bahrami, H. *Desalination.* **2011,** *267*, 64.
24. Wu, F. C.; Tseng, R. L.; Juang, T. S. *J. Hazard. Mater.* **2001,** *81*, 167.
25. WanNgah, W. S.; Ariff, N. F. M.; Hanafiah, M. A .K. M. *Water. Air. Soil. Pollut.* **2010,** *206*, 225.
26. Zhu, H. Y.; Jiang, R.; Xiao, L. *Appl. Clay Sci.* **2010,** *48*, 522.
27. Kittinaovarat, S.; Kansomwan, P.; Jiratumnukul, N. *Appl. Clay Sci* **2010,** *48*, 87.
28. Du, Y.; Zhao, Y.; Dai, S.; Yang, B. *Innov. Food. Sci. Emerg.* **2009,** *10*, 103.
29. Jia, Z.; Shen, D.; Xu, W. *Carbohydr. Res.* **2001,** *333*, 1.
30. Xu, T.; Xin, M.; Li, M.; Huang, H.; Zhou, S.; Liu, J. *Carbohydr. Res.* **2011,** *346*, 2445.
31. Zhao, Z.; Wang, Z.; Ye, N.; Wang, S. *Desalination* **2002,** *144*, 35.
32. Ma, G.; Yang, D.; Zhou, Y.; Xiao, M.; Kennedy, J. F.; Nie, J. *Carbohydr. Polym.* **2008,** *74*, 121.

33. Lagergren, S. About the Theory of so-called Adsorption of Soluble Substance, Kungliga Svenska Vetenskapsakademiens, Handlinger **1898,** Vol *24*, pp 1–39.
34. HO, Y. S.; Mckay, G. *Process Biochem.* **1999,** *34*, 451.
35. Caliskan, N.; Kul, A. R.; Alkan, S.; Sogut, E. G.; Alacabey, I. *J. Hazard. Mater.* **2011,** *193*, 27.
36. Rahchamani, J.; Zavvar Mousavi, H.; Behzad, M. *Desalination* **2011,** *267*, 256.
37. Langmuir, I. *J. Am. Chem. Soc.* **1918,** *40*, 1361.
38. Freundlich H. M. F. *Z. Phys. Chem.* **1906,** *57*, 385.
39. Yu, W.; Lin, J.; Lin, X.; Xie, H.; Zhao, W.; Ma, X. *J. Membr. Sci.* **2010,** *346*, 296.
40. Qin, C. Q.; Du, Y. M.; Xiao, L. *Polym. Degrad. Stab.* **2002,** *76*, 211.
41. Yang-Su, H.; Sang-Hoon, L.; Kyung Ho, C. *J. Phys. Chem. Solids.* **2010,** *71*, 464.
42. Wang, S. F.; Shen, L.; Tong, Y. J.; Chen, L.; Phang, I. Y.; Lim, P. Q.; Liu, T. X. *Polym. Degrad. Stab.* **2005,** *90*, 123.
43. Ennajih, H.; Bouhfid, R.; Essassi, E. M.; Bousmina, M.; Kadib, A. E.; Micropor. *Mesopor. Mat.* **2012,** *152*, 208.
44. Khurana, R.; Coleman, C.; Ionescu-Zanetti, C.; Carter, S. A.; Krishna, V.; Grover, R. K.; Roy, R.; Singh, S. *J. Struct. Biol.* **2005,** *151*, 229.